

## Supporting Information

### Spin engineering of triangulenes and application for nano nonlinear optical materials design

Cui-Cui Yang,<sup>a</sup> Xue-Lian Zheng,<sup>a</sup> Jiu Chen,<sup>a</sup> Wei Quan Tian,<sup>\*a</sup> Wei-Qi Li,<sup>\*bcd</sup> Ling Yang,<sup>\*e</sup>

<sup>a</sup> Chongqing Key Laboratory of Theoretical and Computational Chemistry, College of Chemistry and Chemical Engineering, Chongqing University, Huxi Campus, Chongqing 401331, P. R. China

<sup>b</sup> Department of Physics, Harbin Institute of Technology, Harbin 150001, P. R. China

<sup>c</sup> Technology Innovation Center of Materials and Devices at Extreme Environment, School of Materials Science and Engineering, Harbin Institute of Technology, Harbin 150001, China

<sup>d</sup> Collaborative Innovation Center of Extreme Optics, Shanxi University, Taiyuan 030006, P. R. China

<sup>e</sup> Wenzhou Institute, University of Chinese Academy of Sciences, 1 Jinlian Street, Wenzhou 325001, China

\*Corresponding author: tianwq@cqu.edu.cn; tccliweiqi@hit.edu.cn; yangling@hit.edu.cn

#### Supporting Information list:

**Fig. S1** The structures of (a) B, (b) N, (c) NBN and (d) BNB doped TGn (n=2 to 6). The white, deeppink, black and green denote the hydrogen, boron, carbon and nitrogen atoms, respectively.

**Fig. S2** Evolution of the static first hyperpolarizability ( $\langle\beta_0\rangle$ ) with the numbers of excited states in TG7-BNB-ba.

**Fig. S3** The frontier molecular orbitals of BN doped heptene. The molecular orbitals are predicted with PBE0/6-31G(d,p).

**Fig. S4** The natural atomic spin distributions (spin up: yellow circle, spin down: blue circle) of BN-doped TG7-a/b/ab/ba/c series of molecules and TG7-BNB-ab. Numbers in blue are spin density.

**Fig. S5** The frontier molecular orbitals (plotted with isosurface value of 0.02 a.u.) of TG7 and TG7-ba series of molecules. The molecular orbitals are predicted with PBE0/6-31G(d,p).

**Fig. S6** The transition nature of the electron excitations with major contributions to the  $\langle\beta_0\rangle$  of (a) TG7-B-ba and (b) TG7-N-ba. Molecular orbitals (with isosurface value of 0.02 a.u.) associated with the major electron excitations of these molecules predicted with CAM-B3LYP/6-31++G(d,p).

**Fig. S7** Hole (blue opaque) and electron (yellow opaque) distributions for TG7-B-ba with isosurfaces of 0.0004 and 0.0006 a.u., respectively.

**Fig. S8** Evolution of the  $\langle\beta_0\rangle$  with the electron excitations and the transition nature of the electron excitations with major contributions to the  $\langle\beta_0\rangle$  of TG7-H6-ba, TG7-H6-ba-3NO<sub>2</sub>, TG7-H6-ba-2NO<sub>2</sub>, and TG7-H6-ba-1NO<sub>2</sub>. Hereafter, molecular orbitals (with isosurface value of 0.02 a.u.) associated with the major electron excitations of these molecules predicted with CAM-B3LYP/6-31++G(d,p).  $f$  is the oscillator strength (in a.u.).

**Fig. S9** The transition nature of the electron excitations with major contributions to the  $\langle\beta_0\rangle$  of TG7-NBN-ba.

**Fig. S10** The transition nature of the electron excitations with major contributions to the  $\langle\beta_0\rangle$  of TG7-BNB-ba.

**Fig. S11** The structure of TG7-BNB-ba with Cartesian coordinate, in which the solid line arrow indicates parallel to the paper surface and the dotted arrow indicates outward.

**Fig. S12** The two-dimensional second order nonlinear optical spectra (in  $10^{-30}$  esu) of (a) TG7-B-ba, (b) TG7-N-ba, (c) TG7-NBN-ba, and (d) TG7-BNB-ba scanned up to 7.00 eV with a step size of 0.05 eV.

**Fig. S13** Two-dimensional second order NLO spectra of (a) and (b) TG7-B-ba, (c) and (d) TG7-N-ba, (e) TG7-NBN-ba, and (f) TG7-BNB-ba with step size of 0.005 eV [(a)  $\omega_1$  scanned from 2.50 eV to 3.50 eV and  $\omega_2$  scanned from  $-1.50$  eV to  $-0.50$  eV; (b)  $\omega_1$  scanned from 1.50 eV to 2.50 eV and  $\omega_2$  scanned from 0.50 eV to 1.50 eV; (c)  $\omega_1$  scanned from 1.50 eV to 2.50 eV and  $\omega_2$  scanned from 0.50 eV to 1.50 eV; (d)  $\omega_1$  scanned from 2.50 eV to 3.50 eV and  $\omega_2$  scanned from  $-2.50$  eV to  $-1.50$  eV; (e)  $\omega_1$  scanned from 1.30 eV to 2.30 eV and  $\omega_2$  scanned from  $-0.50$  eV to 0.50 eV; (f)  $\omega_1$  scanned from 1.00 eV to 2.00 eV and  $\omega_2$  scanned from  $-0.50$  eV to 0.50 eV].

**Table S1** The relative electronic energy differences of TGn (n=2 to 7) predicted with (U)PBE0/6-31G(d,p). The doublet in TG2, triplet in TG3, quartet in TG4, quintet in TG5, sextet in TG6, and septet in TG7 are taken as reference, respectively.

**Table S2** The electronic properties including energy gap ( $E_{\text{gap}}$ , in eV) between the highest occupied molecular orbital ( $E_{\text{H}}$ ) and the lowest unoccupied molecular orbital ( $E_{\text{L}}$ ), the lowest vibrational frequency (LVF, in  $\text{cm}^{-1}$ ) and the dipole moment of ground state ( $D_{\text{g}}$ , in Debye), and the static first hyperpolarizability ( $\langle\beta_0\rangle$ , in  $10^{-30}$  esu), the  $\langle\beta_0\rangle$  per heavy atom ( $\langle\beta_0\rangle/N$ ) of TGn (n=2 to 6) series of molecules in closed-shell singlet predicted with PBE0/6-31G(d,p) and TD-CAM-B3LYP/6-31++G(d,p)-SOS, respectively. The relative electronic energy differences ( $\Delta E_{\text{OS-CS}}$  and  $\Delta E_{\text{T-CS}}$ , in Kcal/mol) between open-shell singlet (OS) or triplet (T) and closed-shell singlet (CS) (CS is taken as reference), and spin contamination of open-shell singlet ( $\langle S^2 \rangle$ ) obtained at the UPBE0/6-31G(d,p) level.

**Table S3** Major electronic spectra absorption peaks with transition nature in TG7 series of molecules ( $f$  is the oscillator strength in arbitrary unit,  $E$  is the transition energy in eV unit,  $\lambda$  is the wavelength in nm unit, TNMC to  $\langle\beta_0\rangle$  is the transition nature of electron excitation with major contribution to  $\langle\beta_0\rangle$ ,  $\langle\beta_0\rangle_{\text{con}}$  is contribution value to  $\langle\beta_0\rangle$  in  $10^{-30}$  esu unit).

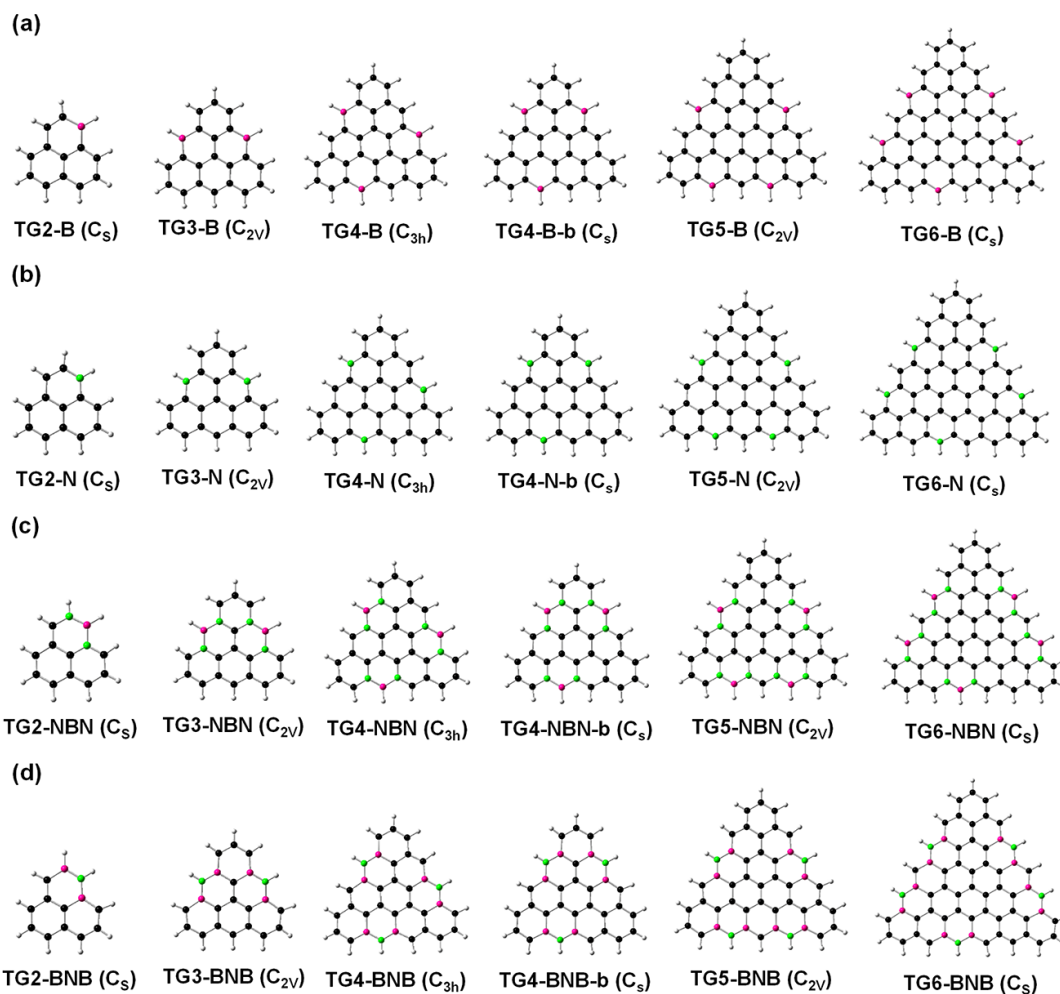


**Fig. S1** The structures of (a) B, (b) N, (c) NBN and (d) BNB doped TGn ( $n=2$  to 6). The white, deeppink, black and green denote the hydrogen, boron, carbon and nitrogen atoms, respectively.

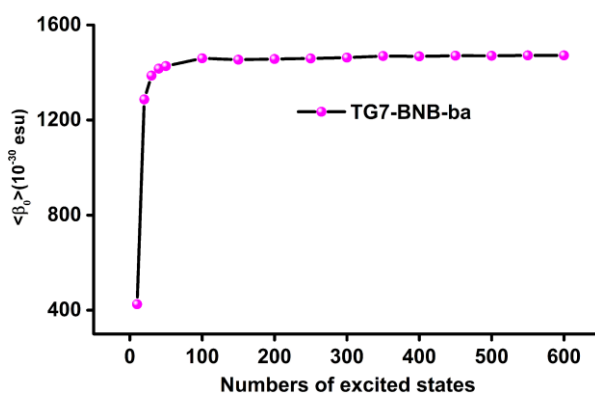


**Fig. S2** Evolution of the static first hyperpolarizability ( $\langle \beta_0 \rangle$ ) with the numbers of excited states in TG7-BNB-ba.

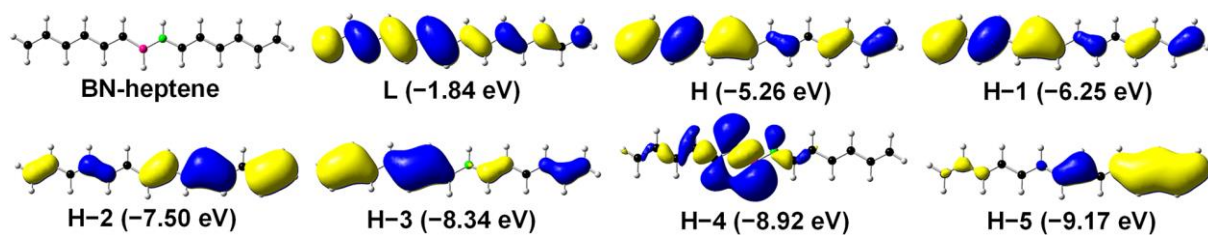


**Fig. S3** The frontier molecular orbitals of BN doped heptene. The molecular orbitals are predicted with PBE0/6-31G(d,p).

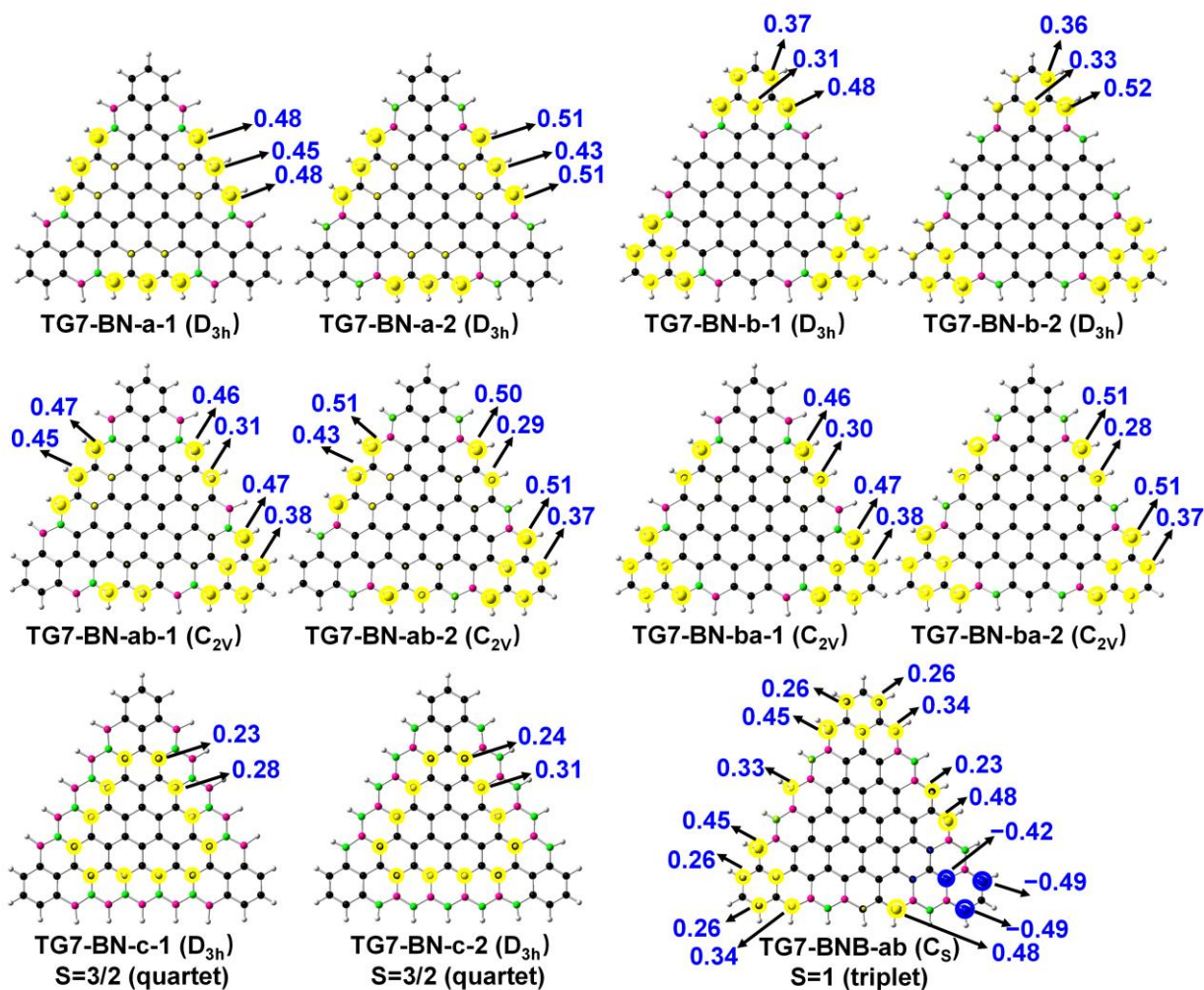


**Fig. S4** The natural atomic spin density distributions (spin up: yellow circle, spin down: blue circle) of BN-doped TG7-a/b/ab/ba/c series of molecules and TG7-BNB-ab. Numbers in blue are spin density.

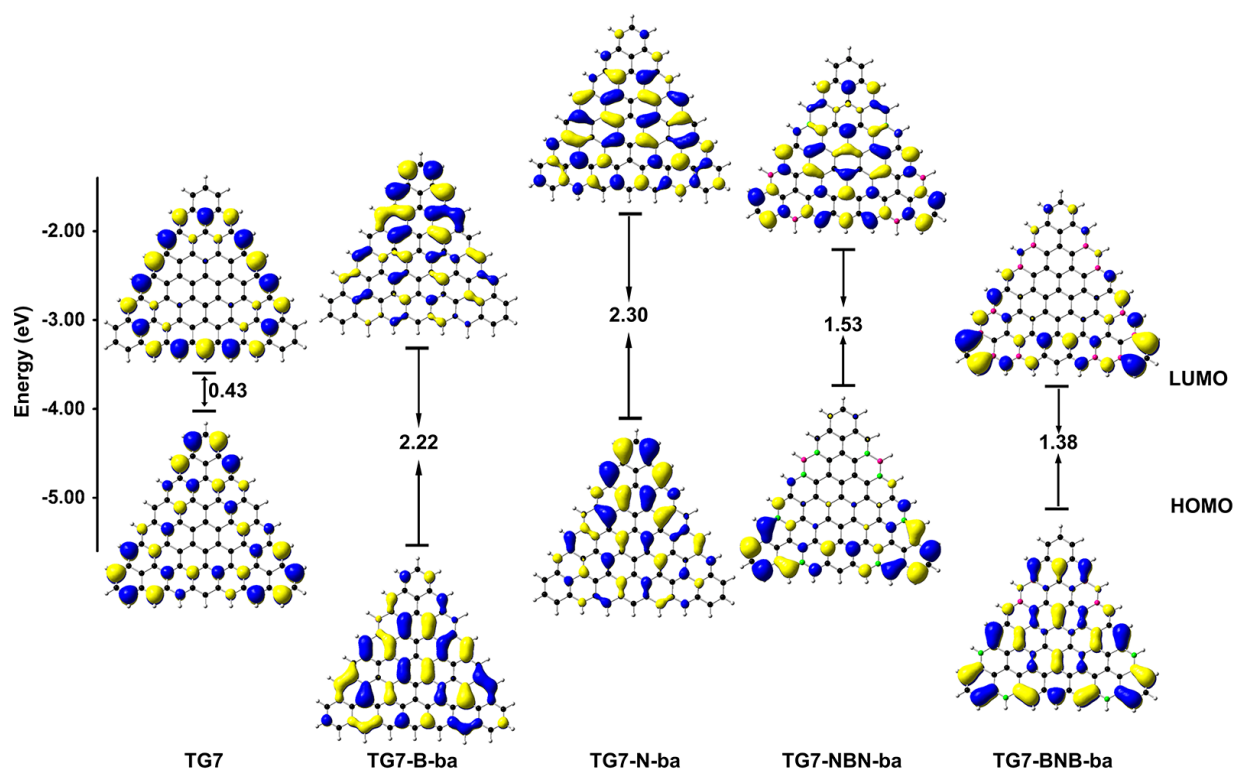


**Fig. S5** The frontier molecular orbitals (plotted with isosurface value of 0.02 a.u.) of TG7 and TG7-ba series of molecules. The molecular orbitals are predicted with PBE0/6-31G(d,p).

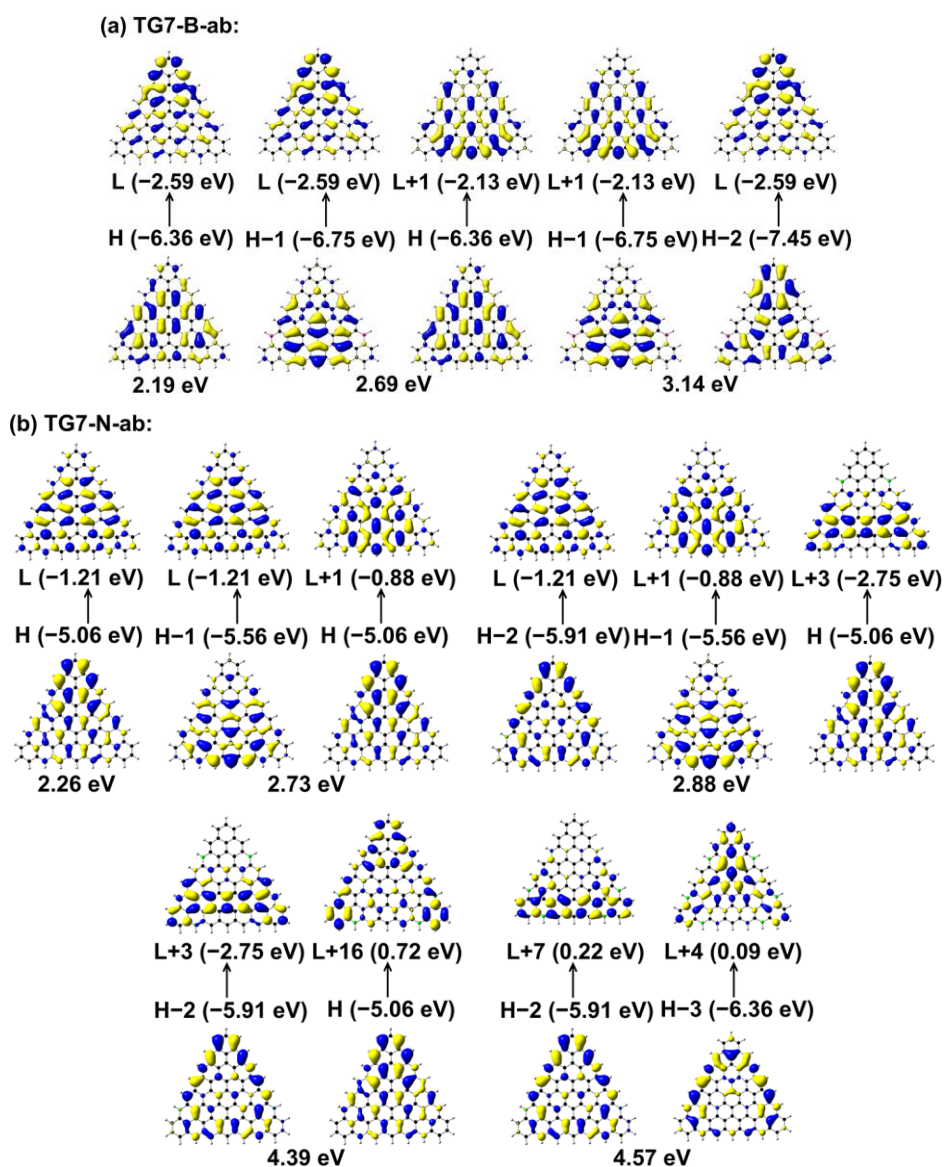


**Fig. S6** The transition nature of the electron excitations with major contributions to the  $\langle\beta_0\rangle$  of (a) TG7-B-ba and (b) TG7-N-ba. Molecular orbitals (with isosurface value of 0.02 a.u.) associated with the major electron excitations of these molecules predicted with CAM-B3LYP/6-31++G(d,p).

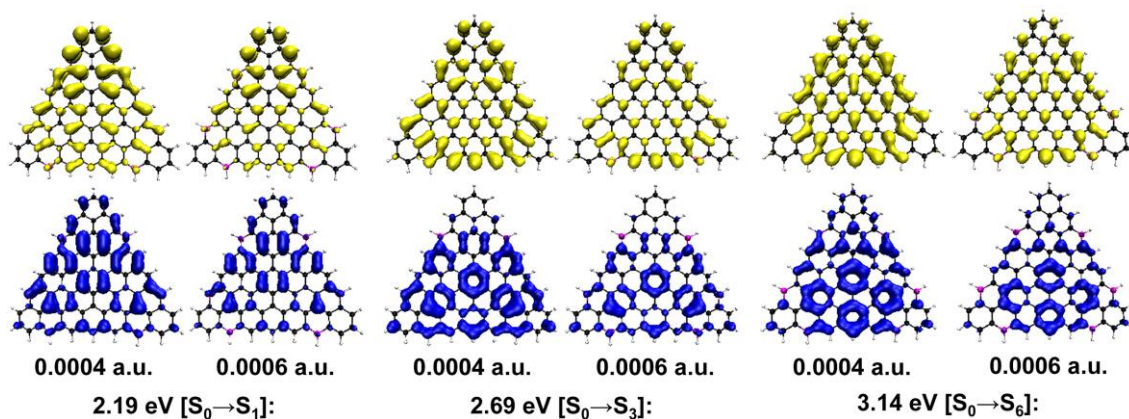


**Fig. S7** Hole (blue opaque) and electron (yellow opaque) distributions for TG7-B-ba with isosurfaces of 0.0004 and 0.0006 a.u., respectively.

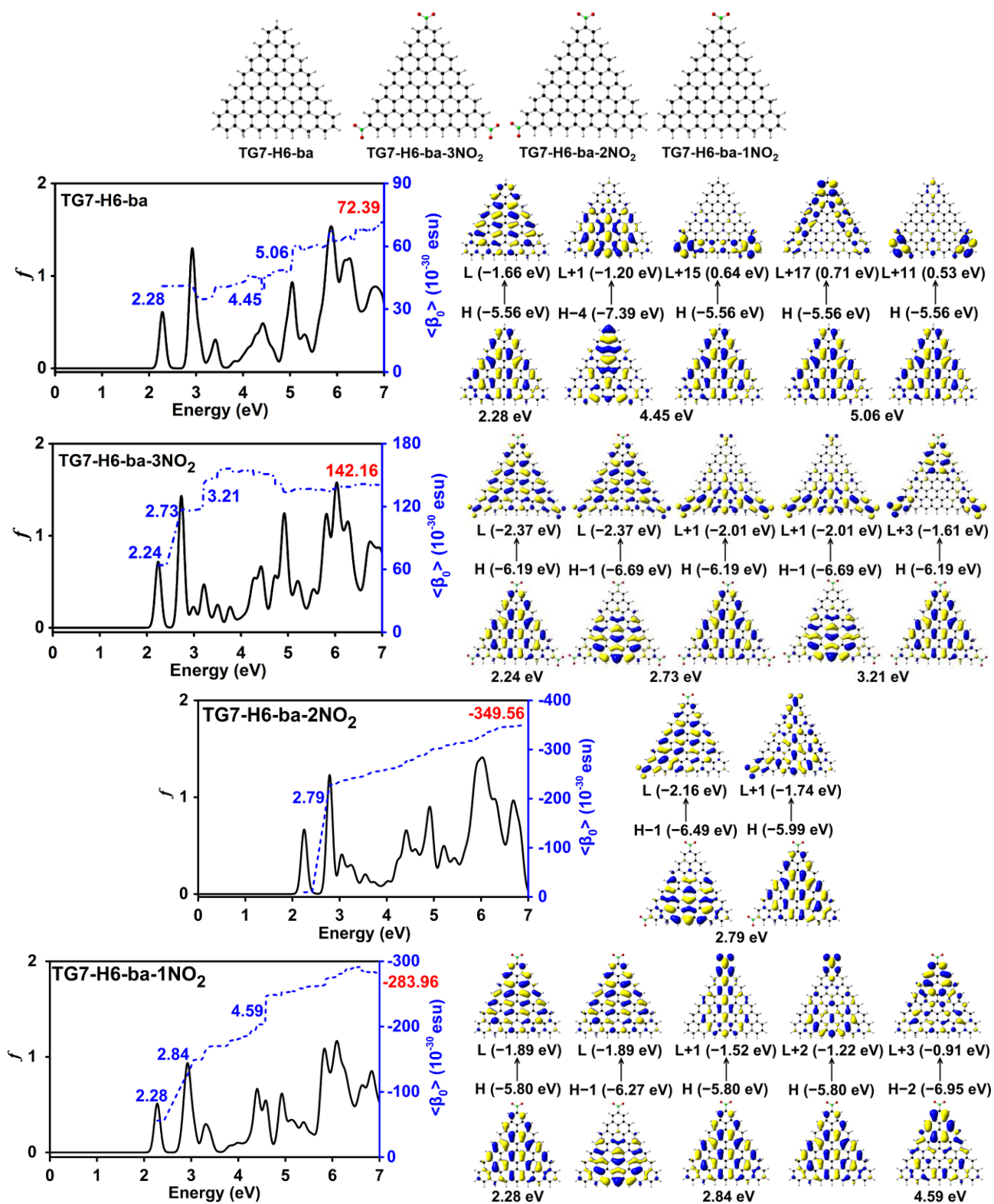


**Fig. S8** Evolution of the  $\langle\beta_0\rangle$  with the electron excitations and the transition nature of the electron excitations with major contributions to the  $\langle\beta_0\rangle$  of TG7-H6-ba, TG7-H6-ba-3NO<sub>2</sub>, TG7-H6-ba-2NO<sub>2</sub>, and TG7-H6-ba-1NO<sub>2</sub>. Hereafter, molecular orbitals (with isosurface value of 0.02 a.u.) associated with the major electron excitations of these molecules predicted with CAM-B3LYP/6-31++G(d,p).  $f$  is the oscillator strength (in a.u.).

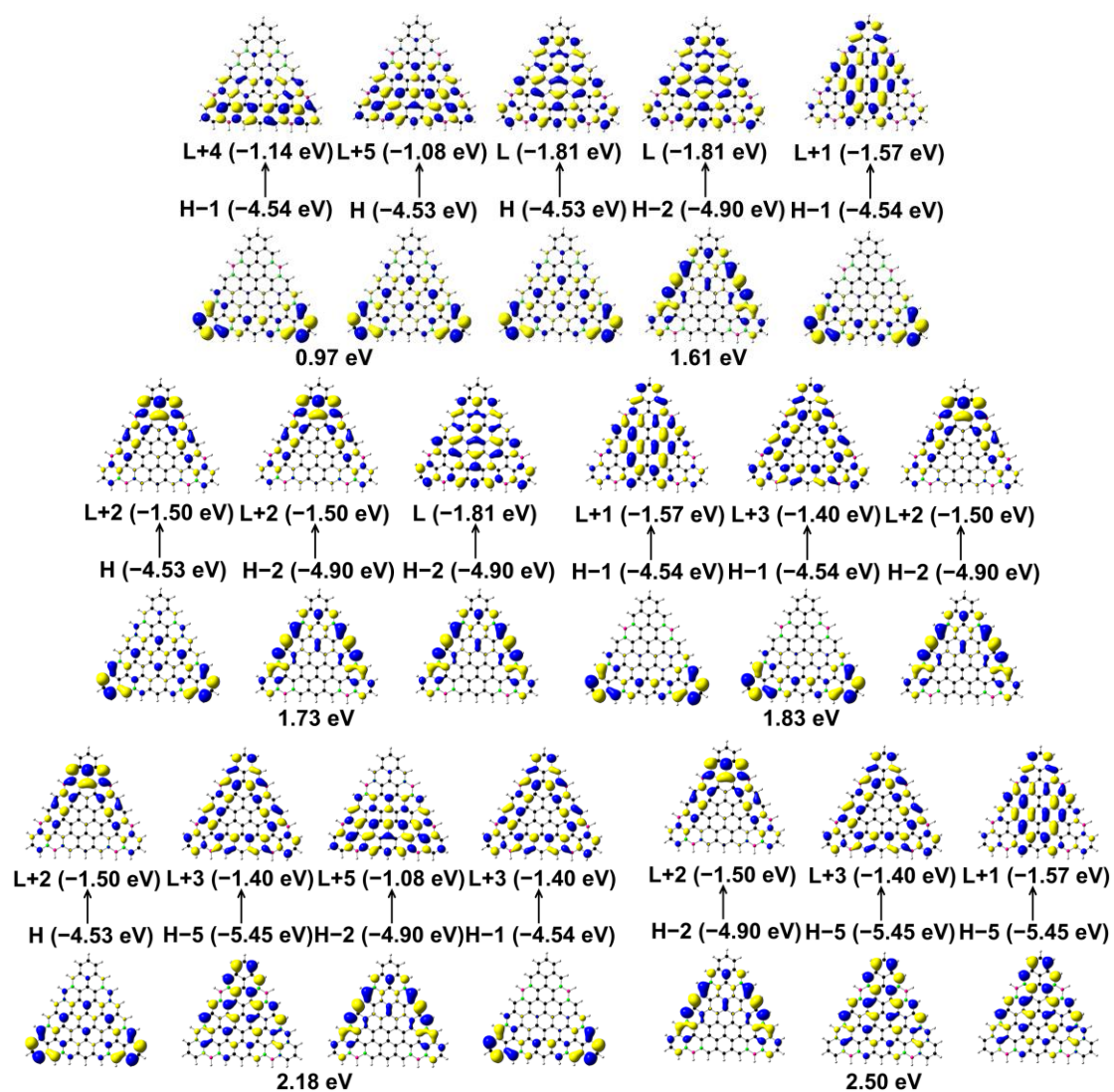


**Fig. S9** The transition nature of the electron excitations with major contributions to the  $\langle\beta_0\rangle$  of TG7-NBN-ba.



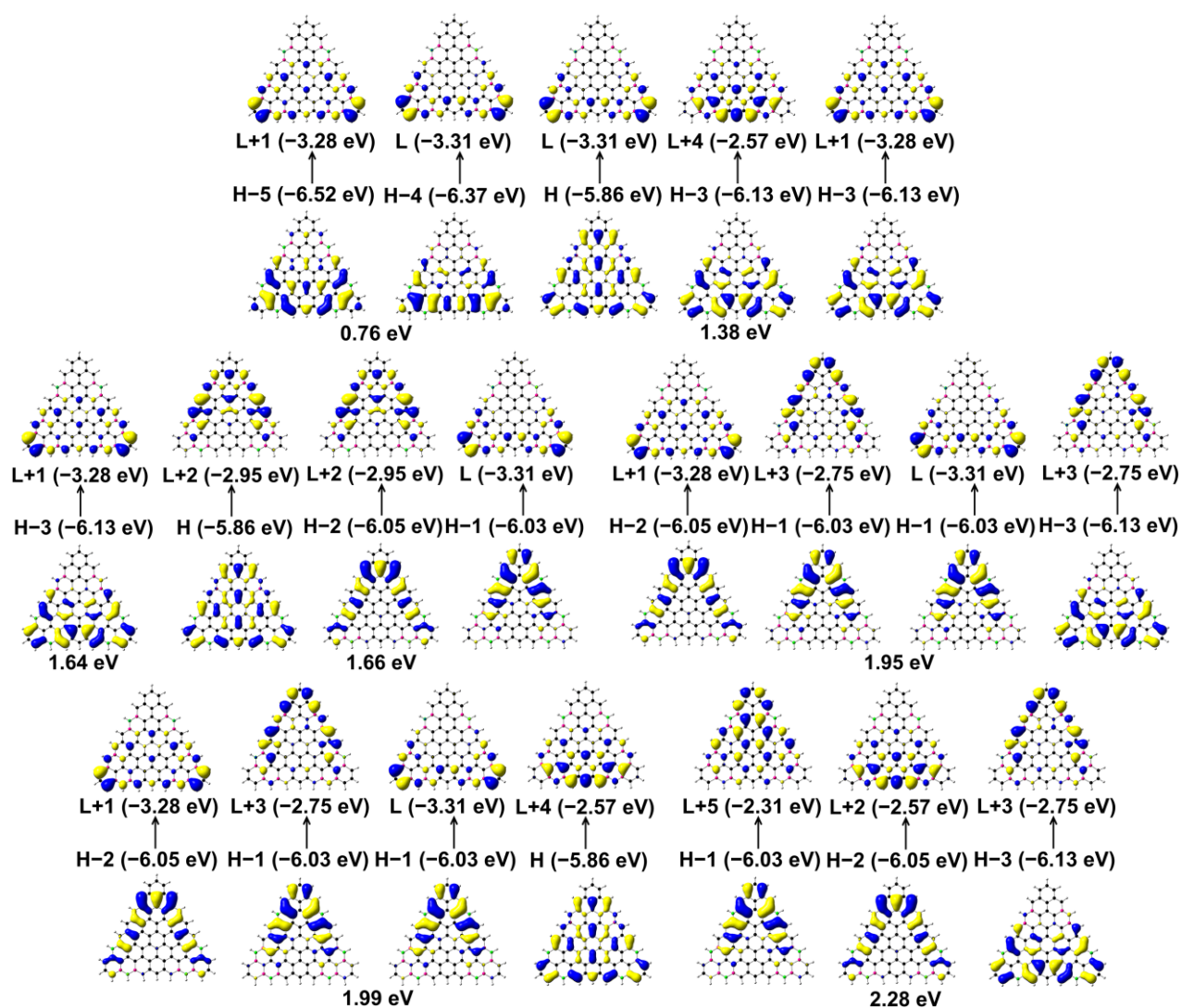


**Fig. S10** The transition nature of the electron excitations with major contributions to the  $\langle\beta_0\rangle$  of TG7-BNB-ba.

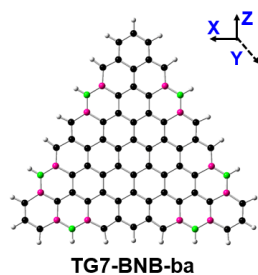


**Fig. S11** The structure of TG7-BNB-ba with Cartesian coordinate, in which the solid line arrow indicates parallel to the paper surface and the dotted arrow indicates outward.

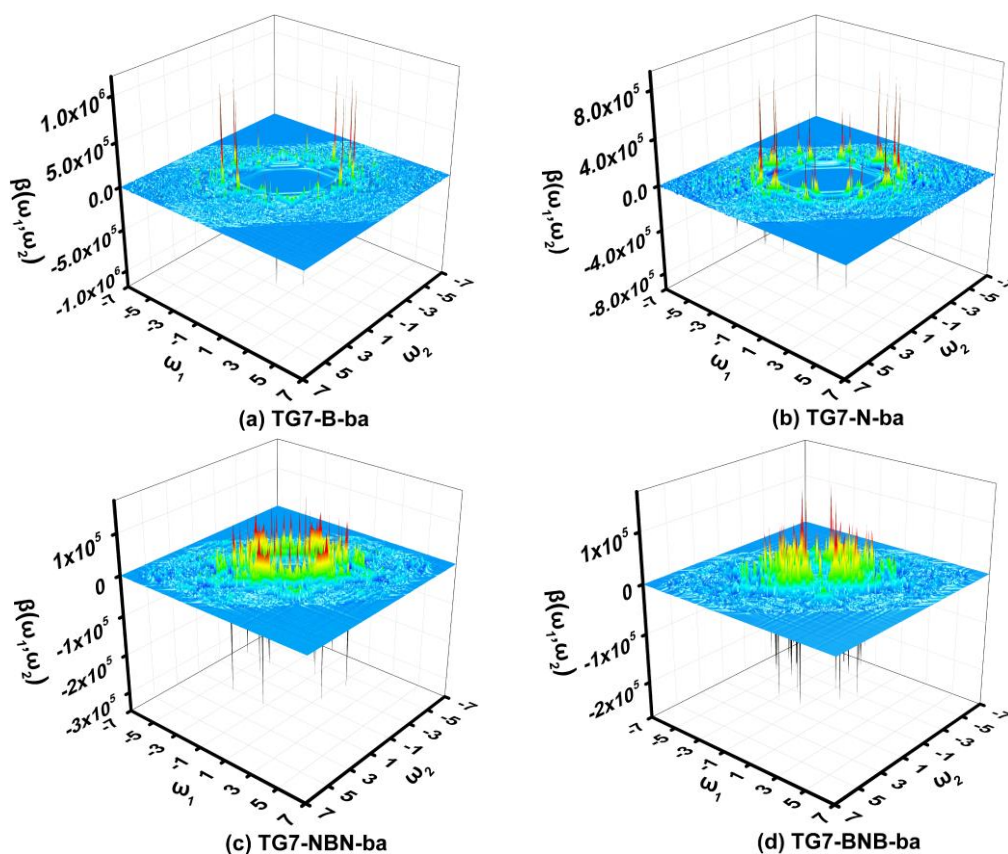


**Fig. S12** The two-dimensional second order nonlinear optical spectra (in  $10^{-30}$  esu) of (a) TG7-B-ba, (b) TG7-N-ba, (c) TG7-NBN-ba, and (d) TG7-BNB-ba scanned up to 7.00 eV with a step size of 0.05 eV.

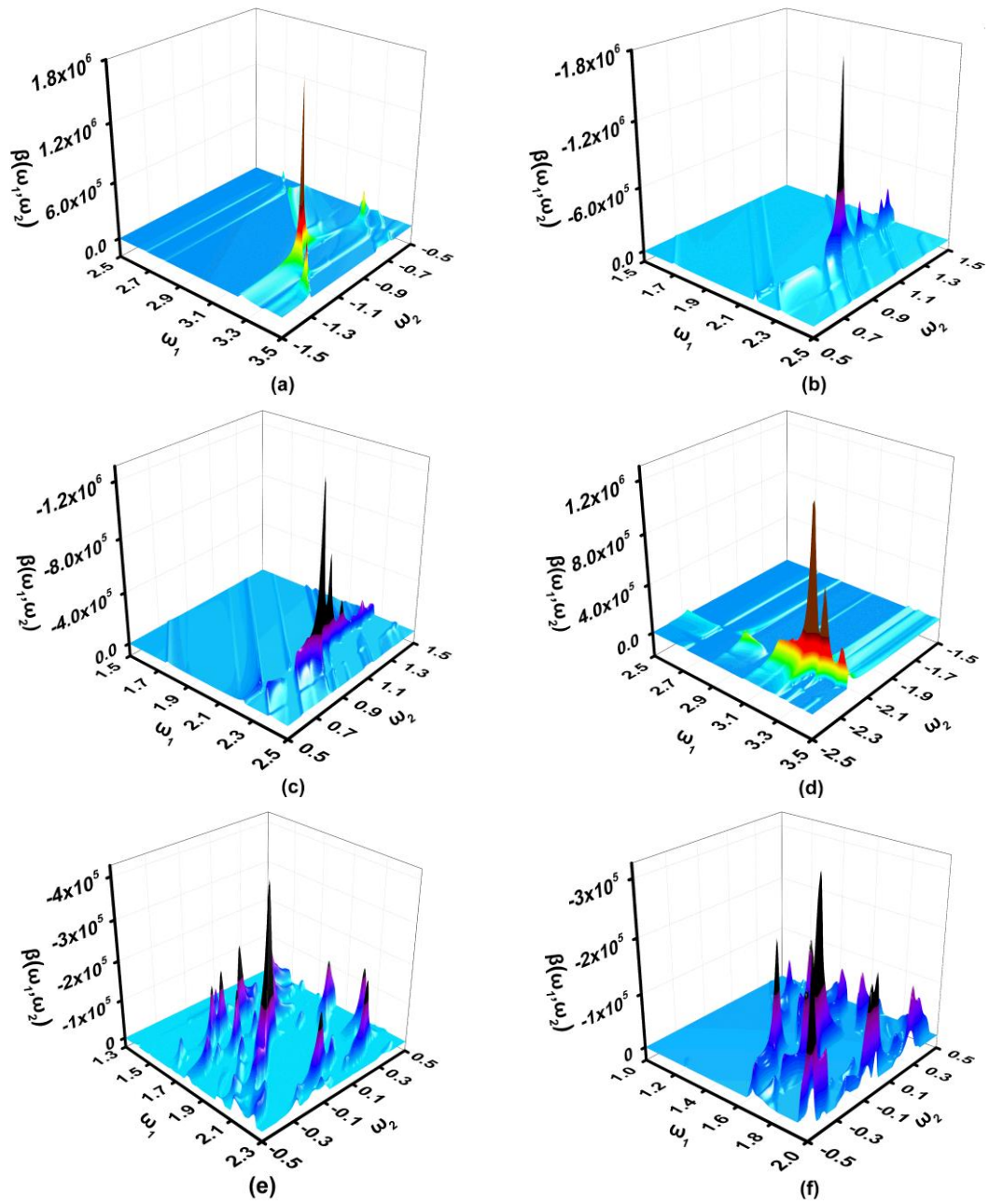


**Fig. S13** Two-dimensional second order NLO spectra of (a) and (b) TG7-B-ba, (c) and (d) TG7-N-ba, (e) TG7-NBN-ba, and (f) TG7-BNB-ba with step size of 0.005 eV [(a)  $\omega_1$  scanned from 2.50 eV to 3.50 eV and  $\omega_2$  scanned from  $-1.50$  eV to  $-0.50$  eV; (b)  $\omega_1$  scanned from 1.50 eV to 2.50 eV and  $\omega_2$  scanned from 0.50 eV to 1.50 eV; (c)  $\omega_1$  scanned from 1.50 eV to 2.50 eV and  $\omega_2$  scanned from 0.50 eV to 1.50 eV; (d)  $\omega_1$  scanned from 2.50 eV to 3.50 eV and  $\omega_2$  scanned from  $-2.50$  eV to  $-1.50$  eV; (e)  $\omega_1$  scanned from 1.30 eV to 2.30 eV and  $\omega_2$  scanned from  $-0.50$  eV to 0.50 eV; (f)  $\omega_1$  scanned from 1.00 eV to 2.00 eV and  $\omega_2$  scanned from  $-0.50$  eV to 0.50 eV].

**Table S1** The relative electronic energy differences of TGn (n=2 to 7) predicted with (U)PBE0/6-31G(d,p). The doublet in TG2, triplet in TG3, quartet in TG4, quintet in TG5, sextet in TG6, and septet in TG7 are taken as reference, respectively.

	TG2	TG4	TG6	TG7-BN-c-1	TG7-BN-c-2
<b>doublet</b>	0.00	18.42	19.05	13.75	5.80
<b>quartet</b>	108.01	0.00	21.08	0.00	0.00
<b>sextet</b>	163.18	80.89	0.00	78.41	67.89
<b>octet</b>	242.47	162.65	79.69	136.18	142.74
	TG3	TG5	TG7	TG7-BNB-ab	
<b>open-shell singlet</b>	6.78	20.36	28.22	7.57	
<b>closed-shell singlet</b>	26.13	46.41	67.77	8.80	
<b>triplet</b>	0.00	9.56	21.21	0.00	
<b>quintet</b>	82.04	0.00	9.47	4.46	
<b>septet</b>	162.24	77.68	0.00	3.97	
<b>nonet</b>	242.05	154.00	72.99	14.79	

**Table S2** The electronic properties including energy gap ( $E_{\text{gap}}$ , in eV) between the highest occupied molecular orbital ( $E_{\text{H}}$ ) and the lowest unoccupied molecular orbital ( $E_{\text{L}}$ ), the lowest vibrational frequency (LVF, in  $\text{cm}^{-1}$ ) and the dipole moment of ground state ( $D_{\text{g}}$ , in Debye), and the static first hyperpolarizability ( $\langle\beta_0\rangle$ , in  $10^{-30}$  esu), the  $\langle\beta_0\rangle$  per heavy atom ( $\langle\beta_0\rangle/N$ ) of TGn (n=2 to 6) series of molecules in closed-shell singlet predicted with PBE0/6-31G(d,p) and TD-CAM-B3LYP/6-31++G(d,p)-SOS, respectively. The relative electronic energy differences ( $\Delta E_{\text{OS-CS}}$  and  $\Delta E_{\text{T-CS}}$ , in Kcal/mol) between open-shell singlet (OS) or triplet (T) and closed-shell singlet (CS) (CS is taken as reference), and spin contamination of open-shell singlet ( $\langle S^2 \rangle$ ) obtained at the UPBE0/6-31G(d,p) level.

Compound	$\Delta E_{\text{OS-CS}}$	$\Delta E_{\text{T-CS}}$	$\langle S^2 \rangle$	LVF	$E_{\text{g}}$	$E_{\text{L}}$	$E_{\text{H}}$	$E_{\text{gap}}$	$\langle\beta_0\rangle$	$\langle\beta_0\rangle/N$
TG2-B	0.00	44.48	0.00	141.74	2.49	-2.33	-6.40	4.07	-4.68	-0.36
TG3-B	0.00	33.17	0.00	71.26	2.85	-2.68	-5.90	3.22	20.34	0.93
TG4-B	0.00	50.56	0.00	44.25	0.00	-2.33	-6.13	3.80	12.85	0.39
TG4-B-b	0.00	34.10	0.00	42.97	2.36	-2.75	-5.81	3.06	68.21	2.07
TG5-B	0.00	32.08	0.00	24.16	4.10	-2.87	-5.67	2.80	92.57	1.52
TG6-B	0.00	33.11	0.00	22.23	1.30	-3.02	-5.64	2.62	23.55	0.37
TG2-N	0.00	46.23	0.00	146.55	2.81	-0.39	-4.62	4.23	-0.83	-0.08
TG3-N	0.00	34.76	0.00	89.70	3.14	-1.06	-4.39	3.33	20.48	0.93
TG4-N	0.00	52.03	0.00	62.65	0.00	-0.98	-4.90	3.92	3.04	0.09
TG4-N-b	0.00	36.17	0.00	62.06	2.85	-1.27	-4.42	3.15	78.03	2.36
TG5-N	0.00	35.04	0.00	42.38	4.65	-1.41	-4.35	2.94	79.87	1.74
TG6-N	0.00	36.11	0.00	30.72	1.49	-1.53	-4.28	2.75	49.99	0.82
TG2-NBN	0.00	5.51	0.00	139.82	2.74	-1.35	-3.65	2.30	22.03	1.69
TG3-NBN	0.00	4.64	0.00	75.19	0.03	-1.59	-3.54	1.95	81.72	3.71
TG4-NBN	0.00	13.19	0.00	53.97	0.00	-1.62	-3.80	2.18	40.33	1.22
TG4-NBN-b	0.00	3.09	0.00	52.98	0.69	-1.84	-3.64	1.80	14.67	0.44
TG5-NBN	0.00	5.04	0.00	39.98	1.98	-1.96	-3.72	1.75	-200.85	4.37
TG6-NBN	0.00	3.71	0.00	29.73	0.19	-2.05	-3.67	1.62	126.48	2.07
TG2-BNB	-4.05	-1.35	0.14	144.00	2.84	-3.37	-5.32	1.95	—	—
TG3-BNB	-8.96	-5.73	2.94	80.54	0.06	-3.58	-5.21	1.63	—	—
TG4-BNB	-1.86	7.36	1.14	48.79	0.00	-3.43	-5.25	1.82	—	—
TG4-BNB-b	-9.87	-7.71	5.70	47.99	0.46	-3.54	-5.10	1.56	—	—
TG5-BNB	-4.47	-5.32	4.26	27.73	1.90	-3.52	-5.01	1.49	—	—
TG6-BNB	-10.43	-10.97	10.29	9.36	0.53	-3.62	-5.03	1.41	—	—

**Table S3** Major electronic spectra absorption peaks with transition nature in TG7 series of molecules ( $f$  is the oscillator strength in arbitrary unit,  $E$  is the transition energy in eV unit,  $\lambda$  is the wavelength in nm unit, TNMC to  $\langle\beta_0\rangle$  is the transition nature of electron excitation with major contribution to  $\langle\beta_0\rangle$ ,  $\langle\beta_0\rangle_{\text{con}}$  is contribution value to  $\langle\beta_0\rangle$  in  $10^{-30}$  esu unit).

Compounds	$f$	$E$	$\lambda$	Transition	TNMC to $\langle\beta_0\rangle$	$\langle\beta_0\rangle_{\text{con}}$
TG7-B-ba (C <sub>72</sub> H <sub>24</sub> B <sub>6</sub> )	0.4972	2.19	566.3	S <sub>0</sub> →S <sub>1</sub>	H→L (87.29%)	236.31
	1.1611	2.69	460.7	S <sub>0</sub> →S <sub>3</sub>	H→L+1 (45.27%) H-1→L (42.57%)	60.43
	0.4314	3.14	395.4	S <sub>0</sub> →S <sub>6</sub>	H-1→L+1 (51.66%) H-2→L (22.79%)	21.80
TG7-N-ba (C <sub>72</sub> H <sub>24</sub> N <sub>6</sub> )	0.4388	2.26	549.5	S <sub>0</sub> →S <sub>1</sub>	H→L (84.25%)	199.88
	0.9443	2.73	454.4	S <sub>0</sub> →S <sub>3</sub>	H-1→L (52.06%) H→L+1 (31.10%) H-2→L (35.62%)	41.19
	0.2178	2.88	430.0	S <sub>0</sub> →S <sub>4</sub>	H-1→L+1 (24.70%) H→L+3 (24.39%)	28.10
	0.1539	3.09	400.9	S <sub>0</sub> →S <sub>6</sub>	H-1→L+1 (36.81%) H→L+3 (36.56%) H-2→L (33.43%)	15.90
	0.6377	3.30	375.7	S <sub>0</sub> →S <sub>9</sub>	H-1→L+1 (22.59%) H-1→L+2 (15.90%) H→L+3 (9.94%) H-2→L (15.93%)	10.49
	0.1831	3.36	368.6	S <sub>0</sub> →S <sub>10</sub>	H-1→L+2 (25.52%) H→L+8 (24.58%) H→L+3 (9.74%)	11.73
	0.4538	3.56	348.0	S <sub>0</sub> →S <sub>14</sub>	H-2→L+1 (26.40%) H→L+10 (14.80%)	17.93
	0.5665	4.39	282.7	S <sub>0</sub> →S <sub>41</sub>	H-2→L+3 (20.66%) H→L+16 (25.84%)	30.18
	0.4901	4.57	271.1	S <sub>0</sub> →S <sub>51</sub>	H-2→L+7 (16.00%) H-3→L+4 (12.80%)	28.30
	TG7-NBN-ba (C <sub>60</sub> H <sub>24</sub> B <sub>6</sub> N <sub>12</sub> )	0.0223	0.97	1273.7	S <sub>0</sub> →S <sub>2</sub>	H-1→L+4 (48.57%) H→L+5 (29.25%) H→L (29.69%)
0.4582		1.61	770.8	S <sub>0</sub> →S <sub>7</sub>	H-2→L (22.03%) H-1→L+1 (13.81%) H→L+2 (38.01%)	135.91
0.0534		1.73	718.3	S <sub>0</sub> →S <sub>9</sub>	H-2→L+2 (20.90%) H-2→L (13.48%) H-1→L+1 (32.52%)	67.66
0.1181		1.83	677.6	S <sub>0</sub> →S <sub>12</sub>	H-1→L+3 (21.95%) H-2→L+2 (15.23%) H→L+2 (18.56%)	239.36
0.1341		2.18	569.6	S <sub>0</sub> →S <sub>21</sub>	H-5→L+3 (14.76%) H-1→L+3 (14.58%) H-2→L+5 (12.96%) H-2→L+2 (22.53%)	108.98
0.6694		2.50	496.6	S <sub>0</sub> →S <sub>31</sub>	H-5→L+3 (17.62%) H-5→L+1 (14.38%)	251.02
TG7-BNB-ba (C <sub>60</sub> H <sub>24</sub> B <sub>12</sub> N <sub>6</sub> )		0.0291	0.76	1622.7	S <sub>0</sub> →S <sub>2</sub>	H-4→L (49.68%) H-5→L+1 (29.26%) H→L (61.28%)
	0.3271	1.38	895.7	S <sub>0</sub> →S <sub>6</sub>	H-3→L+4 (11.50%) H-3→L+1 (11.49%)	126.27

	0.4427	1.64	757.7	$S_0 \rightarrow S_{10}$	H-3→L+1 (47.76%)	112.59
	0.2097	1.66	747.8	$S_0 \rightarrow S_{11}$	H-2→L+2 (28.02%) H-1→L (26.26%) H→L+2 (22.38%)	407.69
	0.3322	1.95	635.1	$S_0 \rightarrow S_{17}$	H-2→L+1 (31.39%) H-1→L+3 (22.38%) H-1→L (13.07%)	211.36
	0.0716	1.99	624.4	$S_0 \rightarrow S_{18}$	H-3→L+3 (11.90%) H-1→L+3 (18.85%) H-2→L+1 (18.71%)	78.97
	0.3265	2.28	544.2	$S_0 \rightarrow S_{27}$	H→L+4 (15.01%) H-1→L (14.52%) H-1→L+5 (35.05%)	52.69
	0.7353	2.28	542.8	$S_0 \rightarrow S_1$	H→L (90.26%)	41.05
TG7-H6-ba (C <sub>78</sub> H <sub>30</sub> )	0.1713	4.45	278.4	$S_0 \rightarrow S_{29}$	H-4→L+1 (17.84%) H→L+15 (15.58%)	6.80
	0.1090	5.06	245.3	$S_0 \rightarrow S_{57}$	H→L+17 (18.97%) H→L+11 (12.82%)	6.88
	0.7906	2.24	553.5	$S_0 \rightarrow S_1$	H→L (88.09%)	63.95
TG7-H6-ba-3NO <sub>2</sub> (C <sub>78</sub> H <sub>27</sub> N <sub>3</sub> O <sub>6</sub> )	1.5789	2.73	453.9	$S_0 \rightarrow S_3$	H-1→L (38.42%) H→L+1 (45.66%)	54.09
	0.4268	3.21	385.7	$S_0 \rightarrow S_7$	H-1→L+1 (30.96%) H→L+3 (25.92%)	25.73
TG7-H6-ba-2NO <sub>2</sub> (C <sub>78</sub> H <sub>28</sub> N <sub>2</sub> O <sub>4</sub> )	1.4120	2.79	444.6	$S_0 \rightarrow S_3$	H-1→L (39.21%) H→L+1 (44.44%)	-218.40
	0.7508	2.28	543.7	$S_0 \rightarrow S_1$	H→L (90.13%)	-56.18
TG7-H6-ba-1NO <sub>2</sub> (C <sub>78</sub> H <sub>29</sub> NO <sub>2</sub> )	0.3907	2.84	436.2	$S_0 \rightarrow S_3$	H-1→L (21.21%) H→L+1 (28.79%)	-61.10
	0.6445	4.59	269.9	$S_0 \rightarrow S_{39}$	H→L+2 (22.82%) H-2→L+3 (13.34%)	-41.80